Spin fluctuations in the ruthenium oxides RuO_2, $SrRuO_3$, $CaRuO_3$, and Sr_2RuO_4 probed by Ru NMR

H. Mukuda
Department of Physical Science, Graduate School of Engineering Science, Osaka University, Toyonaka, Osaka 560-8531, Japan and Core Research for Evolutional Science and Technology (CREST) of the Japan Science and Technology Corporation (JST), Kawaguchi, Saitama 332-0012, Japan

K. Ishida
Department of Physical Science, Graduate School of Engineering Science, Osaka University, Toyonaka, Osaka 560-8531, Japan

Y. Kitaoka
Department of Physical Science, Graduate School of Engineering Science, Osaka University, Toyonaka, Osaka 560-8531, Japan and Core Research for Evolutional Science and Technology (CREST) of the Japan Science and Technology Corporation (JST), Kawaguchi, Saitama 332-0012, Japan

K. Asayama
Department of Physical Science, Graduate School of Engineering Science, Osaka University, Toyonaka, Osaka 560-8531, Japan

R. Kanno
Department of Physics, Faculty of Science, Kobe University, Nada, Kobe, Hyogo 657-8501, Japan

M. Takano
Institute for Chemical Research, Kyoto University, Uji, Kyoto 611-0011, Japan and Core Research for Evolutional Science and Technology (CREST) of the Japan Science and Technology Corporation (JST), Kawaguchi, Saitama 332-0012, Japan

(Received 19 March 1999)

By means of Ru NMR, magnetic properties in three-dimensional (3D) perovskites $SrRuO_3$ (ferromagnet) and $CaRuO_3$ (exchange enhanced paramagnet) were investigated and compared with those in the two-dimensional (2D) layered perovskite Sr_2RuO_4 (superconductor), RuO_2, and Ru metal (Pauli paramagnet). We found that $4d$-spin contributions in the Knight shift and $^{101}(1/T_1)$ of Ru are predominant in $SrRuO_3$, $CaRuO_3$, and Sr_2RuO_4, but not in nonmagnetic RuO_2 and Ru metal. The experimental results that a Stoner factor for $CaRuO_3$ is close to 1 and that a correlation factor estimated from modified-Korringa behavior of Ru-T_1 is much less than 1 indicate that $CaRuO_3$ is a nearly ferromagnetic (FM) metal dominated by low-frequency and long-wavelength components of the spin fluctuations (SF). Even though the Stoner factor for Sr_2RuO_4 also indicates the closeness to the ferromagnetism, the SF in Sr_2RuO_4 are different from those in $CaRuO_3$. The results combined with the previous ^{17}O NMR study in Sr_2RuO_4 indicate that the *in-plane* low-frequency components of SF are exchange enhanced without any significant q dependence due to 2D electronic character (2D nearly FM), while the *out-of-plane* low-frequency component of SF shows the existence of antiferromagnetic (AFM) SF between layers at low temperature. We propose that this evolution from 3D to 2D nearly FM SF is relevant to the onset of spin-triplet superconductivity in Sr_2RuO_4. The 2D nearly FM SF in the in-plane $4d_{xy}$-p_π band may play a significant role for the stabilization of parallel spin pairing state within the basal plane among various representations of spin-triplet order parameter in Sr_2RuO_4. [S0163-1829(99)05041-9]

I. INTRODUCTION

Since the discovery of superconductivity in the copper-free layered perovskite Sr_2RuO_4[1] and the identification of the spin-triplet p-wave superconductivity in the compound,[2] much attention has been paid to the anomalous magnetic and transport properties of Sr_2RuO_4 and related ruthenium oxides. A series of ruthenium oxides $(Sr,Ca)_{n+1}Ru_nO_{3n+1}$ have been known to show rich properties: a ferromagnetic (FM) metal, an antiferromagnetic (AFM) insulator and a superconductor. Especially, understanding of their magnetic properties in these ruthenates allows us to gain insight into the occurrence of the spin-triplet superconductivity in Sr_2RuO_4. $SrRuO_3$ and $CaRuO_3$, which are $n=\infty$ members of the series, have nearly cubic and slightly distorted cubic perovskite structure, respectively. Although both the ruthenates exhibit metallic behavior,[3,4] their magnetic properties are quite different: $SrRuO_3$ is a FM metal with the Curie temperature $T_C=160$ K,[5,6] whereas $CaRuO_3$ does not show any magnetic anomalies even at low temperature (T).[7] The Ca substitution for the Sr sites makes the RuO_6 octahedra tilt slightly from the c axis and rotates around it to fill the extra space of Sr-shared positions, since an ionic radius of Ca is smaller than of Sr. However, each RuO_6 octahedron is not distorted, then, the angle of Ru-O-Ru bond connecting octahedra directly influences the bandwidth of $dp\pi^*$ state. With

increasing the Ca substitution for the Sr sites in $Sr_{1-x}Ca_xRuO_3$, T_C decreases rapidly and no magnetic order is found in $x \geqslant 0.7$, whereas the Curie constant is nearly independent of the Ca concentration.[8,4] Although the AFM interaction of $CaRuO_3$ is inferred from the large negative value of the Weiss temperature in the framework of local moment model, any trace of AFM correlation is not evidenced by experiments. While $Sr_{1-x}Ca_xRuO_3$ conserves the metallic conductivity down to lowest T without depending Ca content,[3,4] the other pseudoternary ruthenates $Sr_{2-x}Ca_xRuO_4$ $(n=1)$ (Ref. 9) and $Sr_{3-x}Ca_xRu_2O_7$ $(n=2)$ (Refs. 10 and 11) show a metal-insulator transition with increasing the Ca content. The end members Ca_2RuO_4 and $Ca_3Ru_2O_7$ are the AFM-Mott insulators.[9–11] In contrast, a magnetic ground state of $CaRuO_3$ is still not clear to date.

Pauli-paramagnetic compound RuO_2 with the rutile structure[12] is also a good reference compound to understand the magnetic properties in the RuO_6 octahedron. The electron configuration in the RuO_2 having the distorted octahedral structure is $4d^{4+}(t_{2g}^4 e_g^0)$ which is analogous to that in the series of $(Sr,Ca)_{n+1}Ru_nO_{3n+1}$. Note, however, that the edge sharing of the RuO_6 octahedra makes conductivity better because of the larger $4d(t_{2g})$-p_π hybridization through nearly the 90° Ru-O-Ru bridgelike bond[13] than the corner sharing through nearly the 180° Ru-O-Ru linear bond. Consequently, RuO_2 exhibits a T-independent susceptibility.[14]

In this paper, we report systematic Ru-NMR studies for $SrRuO_3$, $CaRuO_3$, and RuO_2 as well as Ru metal, and compare these results with those reported on the 2D-layered perovskite Sr_2RuO_4.[15] We show that $CaRuO_3$ is entitled as a 3D nearly FM metal with a Stoner factor $\alpha \approx 0.98$, whereas Sr_2RuO_4 as a quasi-2D exchange enhanced metal. We found that spin fluctuations (SF) in $CaRuO_3$ are dominated by low-frequency and long-wavelength components, whereas the SF in Sr_2RuO_4 reveals a weak wave-number dependence associated with the quasi-2D electronic character. In this sense, it is emphasized that the occurrence of the spin-triplet p-wave superconductivity in Sr_2RuO_4 does not always originate from the 3D-FM SF with analogy to liquid ^{3}He. Alternatively, the 2D nearly FM SF in the in-plane $4d_{xy}$-p_π band may play a significant role for the stabilization of parallel spin pairing state within the basal plane[2] among various representations of spin-triplet order parameter.

II. EXPERIMENTAL PROCEDURES

Powdered samples of Ru metal (Ru > 99.98% purity) and RuO_2 (RuO_2 > 99.9% purity) were used for NMR measurements. $SrRuO_3$ and $CaRuO_3$ were prepared by heating appropriate molar ratios of $SrCO_3$, $CaCO_3$, and RuO_2 with $3N$ purity, and calcined at 1223 K for 24 h.[3] After reground, the samples were pressed into pellets again and fired at 1473 K for 24 h. The powdered samples of $SrRuO_3$ and $CaRuO_3$ were used for magnetization and NMR measurements. The magnetization measurements for $SrRuO_3$ and $CaRuO_3$ were performed under the magnetic field $H=1$ kOe, using a superconducting quantum interference device (SQUID) magnetometer. The Curie temperature T_C of $SrRuO_3$ is 160 K and an effective paramagnetic moment p_{eff} above T_C is $2.68\mu_B$. $CaRuO_3$ has a negative large Weiss temperature $\theta = -137 \pm 10$ K without exhibiting any magnetic transition down to 1.4 K and p_{eff} is estimated as $3.15\mu_B$ in $T=100$–300 K. These results indicate that the Ru ion is in the tetravalent state $(4d)^{4+}(t_{2g}^4 e_g^0)$ for the low-spin state $(S=1)$, since p_{eff}'s for both the ruthenates are close to $2\mu_B\sqrt{S(S+1)} = 2.83\mu_B$ $(S=1)$.

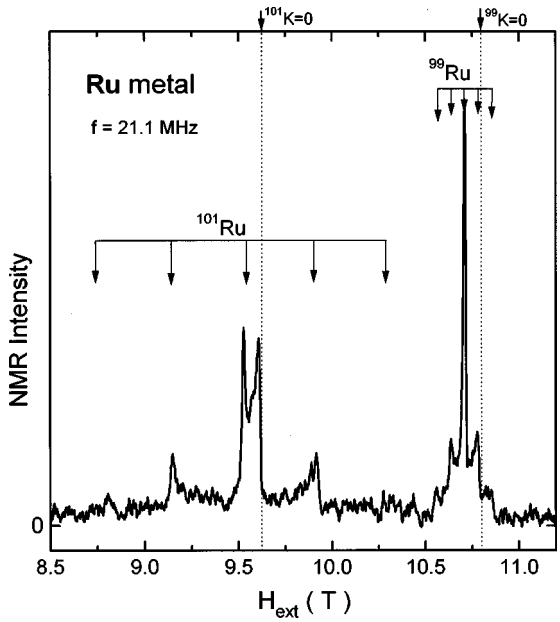

FIG. 1. The Ru-NMR spectrum of hcp Ru metal. Peaks at a lower (higher) field side corresponds to ^{101}Ru- (^{99}Ru-) NMR spectrum articulated by the electric quadrupole interaction.

Spin-echo NMR measurements were performed using a conventional phase-coherent-type spectrometer. Nuclear-spin-lattice relaxation time T_1 was obtained by means of the saturation-recovery method. T_1 for all compounds was determined with a single component by fitting the recovery of nuclear magnetization to the following relaxation function for $I=5/2$:[16]

$$\frac{M(\infty)-M(t)}{M(\infty)} = 0.028\exp\left(-\frac{t}{T_1}\right) + 0.178\exp\left(-\frac{6t}{T_1}\right) + 0.794\exp\left(-\frac{15t}{T_1}\right). \quad (1)$$

III. RESULTS AND DISCUSSIONS

A. Ru metal

Figure 1 indicates the NMR spectrum of ^{99,101}Ru ($I=5/2$) in Ru metal with the hexagonal close-packed structure. The spectrum at a low- (high-) field side exhibits a typical powder pattern for ^{101}Ru (^{99}Ru) which is well articulated by the nuclear electric quadrupole (eqQ) interaction. The nuclear quadrupole resonance frequency ν_Q of ^{99}Ru (^{101}Ru) is estimated to be 0.29 (1.68) MHz.

The Knight shift K_x, K_y, and K_z along x, y, and z axes, is estimated to be +0.64%, +0.64%, and +0.73%, being T independent in $T=1.4$–20 K. The isotropic (anisotropic) part of the Knight shift, $K_{iso}=(K_x+K_y+K_z)/3$ $[K_{aniso}=(2K_z-K_x-K_y)/6]$, is estimated to be +0.67% (+0.03%). The

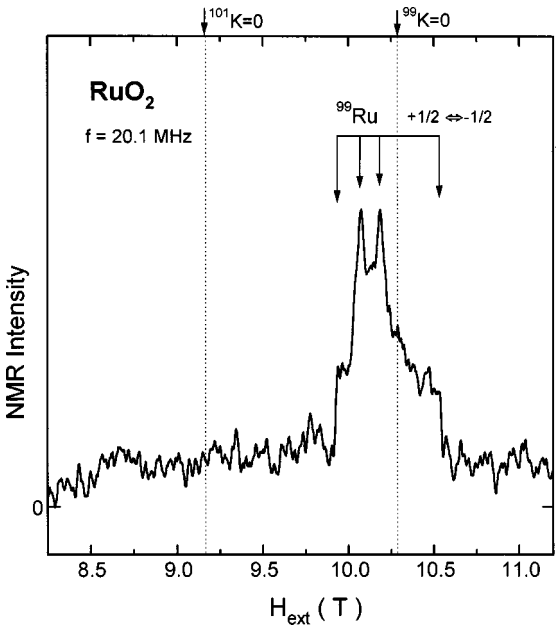

FIG. 2. The Ru-NMR spectrum of RuO_2 with the rutile structure. This spectrum arises from the $\phi(+1/2)\Leftrightarrow\phi(-1/2)$ transition affected by the nuclear electric quadrupole interaction with a large asymmetric parameter η. Arrows denote resonance fields where two peaks and edges appear in a powder pattern. They are calculated using $\eta\sim0.74$ and $^{99}\nu_Q\sim3.18$ MHz.

T-independent $K_{\rm iso}$ with a positive value is due to dominance of the $4d$ orbital and/or the $5s$ contributions, consistent with the previous report.[17]

Figure 6 indicates the T dependence of $^{101}(1/T_1)$ that follows a T-linear behavior. A constant value of $^{101}(T_1T)^{-1}$ is two orders of magnitude smaller than that reported in Sr_2RuO_4.[15] Apparently, a dominant relaxation process in the Ru metal is not open to the $4d$-spin channel, but to the $4d$-orbital and/or the $5s$-spin channels.

B. RuO_2

Figure 2 shows the ^{99}Ru-NMR spectrum arising from the $\phi(+1/2)\Leftrightarrow\phi(-1/2)$ transition affected by the eqQ interaction with a large asymmetric parameter η. Arrows denote resonance fields where two peaks and edges appear in a powder pattern. They are calculated using $\eta\sim0.74$ and $^{99}\nu_Q\sim3.18$ MHz. The articulated spectral structure from other satellite peaks for ^{99}Ru was not observed due to smearing out by large η, and the entire spectrum for ^{101}Ru was not detectable due to the broadening by the large eqQ interaction originating from large nuclear quadrupole moment, ^{101}Q of ^{101}Ru ($^{101}Q/^{99}Q\sim5.8$). The large value of η is associated with the distorted structure in the RuO_6 octahedron.[18]

The Knight shift $K_{\rm obs}$ is T independent with a positive value of $+1.59\%$ in $T=1.4$–20 K. It should be noted that $K_{\rm obs}=1.59\%$ is comparable to an estimated value of the orbital Knight shift $K_{\rm orb}\sim1.08\%$ in Sr_2RuO_4.[15] $^{99}(T_1T)^{-1}$ stays constant in $T=1.4$–20 K. In Fig. 6, $^{101}(T_1T)^{-1}$ estimated from the relation of $(^{101}\gamma_n/^{99}\gamma_n)^2\cdot{}^{99}(T_1T)^{-1}$ is plotted, being comparable with the value in Ru metal. Since an orbital contribution in $^{101}(T_1T)^{-1}$ is negligibly smaller than a value calculated using the density of states,[19] $^{101}(T_1T)^{-1}$ is hence expected to be dominated by the $5s$-spin contribution. In RuO_2, the $4d$-spin contribution is not seen in the Knight shift and $^{101}(1/T_1)$ as well as in Ru metal.

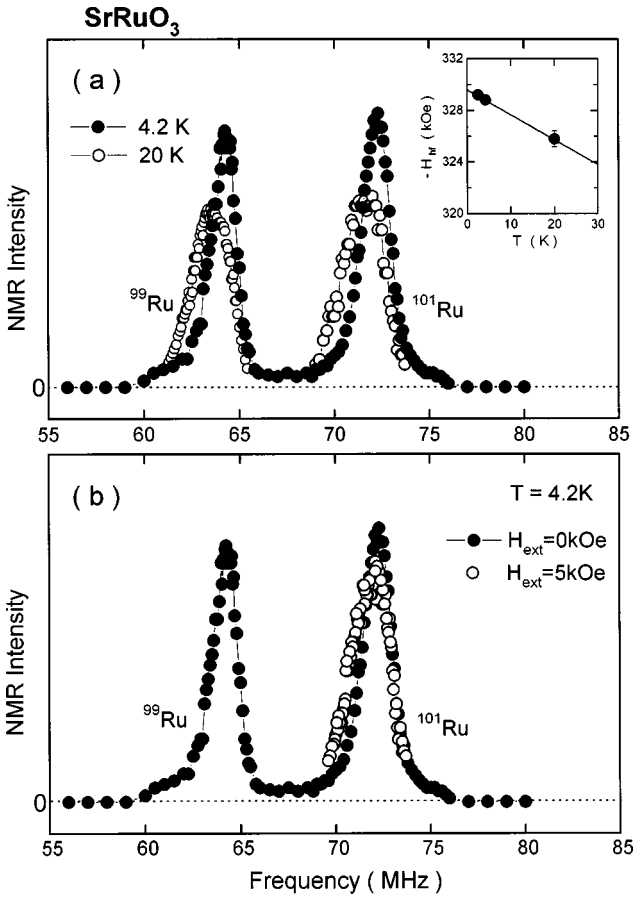

FIG. 3. The Ru-NMR spectra in the ferromagnetic state of $SrRuO_3$ at zero field (a) at 4.2 and 20 K. The hyperfine field $H_{\rm hf}$ extrapolated to $T\rightarrow0$ K is estimated to be -329.6 kOe from $H_{\rm hf}$ vs T plot in the inset. (b) The spectra at the magnetic field $H_{\rm ext}=0$ and 5 kOe. Application of small external field makes the spectrum shift to lower frequency side, which evidences the negative sign of $H_{\rm hf}$.

C. $SrRuO_3$

Figure 3(a) indicates the Ru-NMR spectra at zero field in the FM state at 4.2 and 20 K. The ratio of two resonance frequencies 72.3/64.2 MHz is equivalent to the ratio of the gyromagnetic ratio, $^{101}\gamma_n/^{99}\gamma_n=1.12$, and an intensity ratio is nearly the same as the ratio of the natural abundance (NA) for the two isotopes, $^{101}{\rm NA}/^{99}{\rm NA}=1.35$. Therefore two peaks arise from ^{99}Ru and ^{101}Ru with the same internal hyperfine field $H_{\rm hf}$. Note that their spectral widths are magnetic in origin. If a possible distribution of electric-field gradient were responsible for their spectral broadening, a ratio of width should follow the ratio of nuclear quadrupole moment $^{101}Q/^{99}Q=5.8$. This is not the case, in fact. Application of small external field makes the spectrum shift to lower frequency side as indicated in Fig. 3(b), which evidences the negative sign of $H_{\rm hf}$. The spectrum slightly shifts to lower frequency side upon heating as indicated in Fig. 3(a). An averaged value of $H_{\rm hf}$ is estimated to be -329.6 kOe from an extrapolation to $T\rightarrow0$ K as in the inset of the figure.

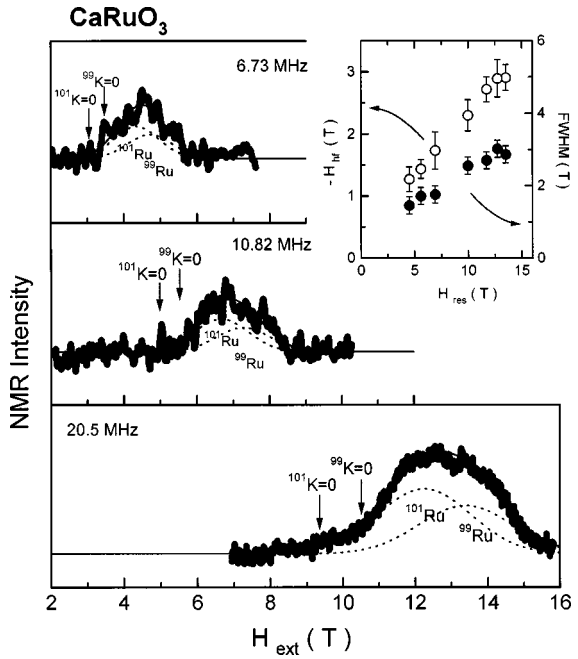

FIG. 4. The Ru-NMR spectra at three frequencies $f=6.73$, 10.82, and 20.5 MHz and at 4.2 K. These spectra are widely broadened with a large $K_{\rm obs}$. All the spectra are well reproduced by two Gaussian ^{99}Ru and ^{101}Ru spectra as fit by dashed lines. We assumed that the total-intensity ratio and FWHM ratio of the two Gaussians are fixed to ^{101}NA/^{99}NA$=1.35$ and $^{101}\gamma_{\rm n}/^{99}\gamma_{\rm n}=1.12$, respectively. FWHM and $H_{\rm hf}$ are fitting parameters. As seen in the inset, the magnitudes of $H_{\rm hf}$ and FWHM increase as $H_{\rm res}$ increases.

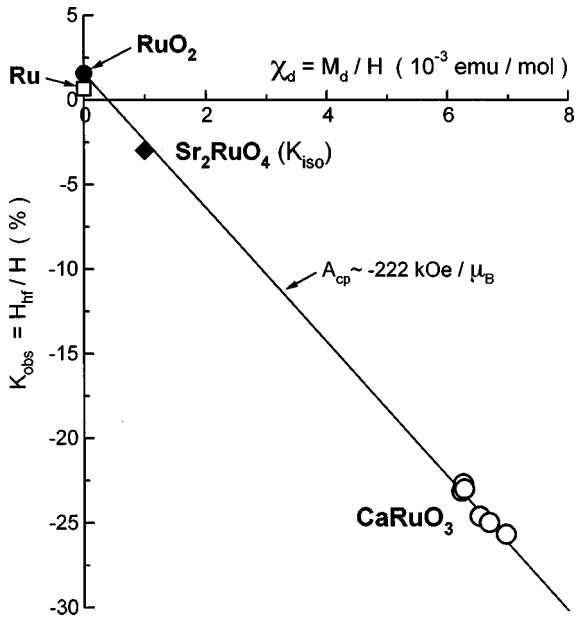

FIG. 5. Knight shift vs susceptibility $[M_{\rm d}(H)/H]$ with an implicit parameter of the external field H. The hyperfine coupling constant due to the inner core polarization $A_{\rm cp}\approx -222\pm 50$ kOe/$\mu_{\rm B}$ is estimated from a slope of linear line when $K_{5s}+K_{\rm orb}$ is assumed to be the same value as $K_{\rm obs}=+1.59\%$ in RuO_2. This value is close to $A_{\rm hf}\sim -300\pm 60$ kOe/$\mu_{\rm B}$ in the FM state of $SrRuO_3$. Note that the Knight shift for Sr_2RuO_4 lies on the same line of $K_{\rm obs}$ vs $\chi_{\rm obs}$ plot as that for $CaRuO_3$.

The $H_{\rm hf}$ in $4d$-transition metals is expressed to be $H_{\rm hf}=(A_{\rm hf}/N_{\rm A}\mu_{\rm B})M_0$, where $A_{\rm hf}$, $N_{\rm A}$, and M_0 are the hyperfine coupling constant, the Avogadro's number, and the FM saturation moment, respectively. If we use $M_0\sim 1.1\pm 0.4\mu_{\rm B}$ reported in the literatures,[6,20] $A_{\rm hf}$ is estimated to be about -300 ± 60 kOe/$\mu_{\rm B}$ in the FM state which is close to that for a Ru impurity in the FM state of Fe.[21]

D. $CaRuO_3$

1. NMR spectrum and Knight shift

Figure 4 indicates the Ru-NMR spectra at three frequencies $f=6.73$, 10.82, and 20.5 MHz, which are widely broadened with a large $K_{\rm obs}$ at 4.2 K. These spectral widths with no structure increase as frequency f or magnetic field $H_{\rm res}$ increases. Here $^{99,101}H_{\rm res}=f/^{99,101}\gamma_{\rm n}-H_{\rm hf}$. This is in contrast to the case for the nonmagnetic Ru metal and RuO_2. The increase in full width at half maximum (FWHM) with increasing $H_{\rm res}$ does not originate from the eqQ interaction, but mainly from $K_{\rm aniso}$. This is because if FWHM originated from the eqQ interaction, FWHM $\propto 1/H_{\rm res}$ should be expected. All the spectra are well reproduced by two Gaussian ^{99}Ru and ^{101}Ru spectra as indicated in Fig. 4. The total-intensity ratio and FWHM ratio of the two Gaussians are fixed to ^{101}NA/^{99}NA$=1.35$ and $^{101}\gamma_{\rm n}/^{99}\gamma_{\rm n}=1.12$, respectively. FWHM and $H_{\rm hf}$ are fitting parameters. As seen in the inset, the magnitudes of $H_{\rm hf}$ and FWHM increase as $H_{\rm res}$ increases.

In general, magnetization under magnetic field H, $M_{\rm obs}(H)$ consisting of $5s$-spin, $4d$-orbital, and $4d$-spin $(M_{\rm d})$ contributions is given by

$$M_{\rm obs}(H)=(\chi_{5s}+\chi_{\rm orb})H+M_{\rm d}(H). \tag{2}$$

The hyperfine field $H_{\rm hf}$ at the Ru site is also expressed by the sum of the $5s$-spin (H_{5s}), the $4d$-orbital $(H_{\rm orb})$, and the $4d$-spin $(H_{\rm d})$ contributions as

$$H_{\rm hf}=H_{5s}+H_{\rm orb}+H_{\rm d}=\left(\frac{A_{5s}}{N_{\rm A}\mu_{\rm B}}\chi_{5s}+\frac{A_{\rm orb}}{N_{\rm A}\mu_{\rm B}}\chi_{\rm orb}\right)H$$
$$+\frac{A_{\rm cp}}{N_{\rm A}\mu_{\rm B}}M_{\rm d}(H)=(K_{5s}+K_{\rm orb})H+\frac{A_{\rm cp}}{N_{\rm A}\mu_{\rm B}}M_{\rm d}(H), \tag{3}$$

where $K_i=(A_i/N_{\rm A}\mu_{\rm B})\chi_i$ $(i=5s$, orb, and $d)$, and the hyperfine-coupling constant $A_{\rm cp}$ is due to the inner-core polarization induced by $4d$ spins. From Eq. (3), the Knight shift $K_{\rm obs}$ at the Ru site is given by

$$K_{\rm obs}=\frac{H_{\rm hf}}{H}=K_{5s}+K_{\rm orb}+\frac{A_{\rm cp}}{N_{\rm A}\mu_{\rm B}}\frac{M_{\rm d}(H)}{H}. \tag{4}$$

As shown in Fig. 5, $K_{\rm obs}$ is plotted against $M_{\rm d}(H)/H$ for $CaRuO_3$ with an implicit parameter of H. Here $\chi_{5s}+\chi_{\rm orb}$ is assumed to be T-independent part in Curie-Weiss behavior $[\chi_0\sim 0.7\times 10^{-3}$ (emu/mol) (Ref. 4)], and then $M_{\rm d}(H)$ is estimated by subtracting $\chi_0 H$ from the observed magnetization $M_{\rm obs}$ (Ref. 4) in Eq. (2). If we assume $K_{5s}+K_{\rm orb}$ in Eq. (4) to be the same value as $K_{\rm obs}=+1.59\%$ in RuO_2, $A_{\rm cp}\approx -222\pm 50$ kOe/$\mu_{\rm B}$ is estimated from a slope in Fig. 5. This value is between -345 kOe/$\mu_{\rm B}$ (Pd metal) and

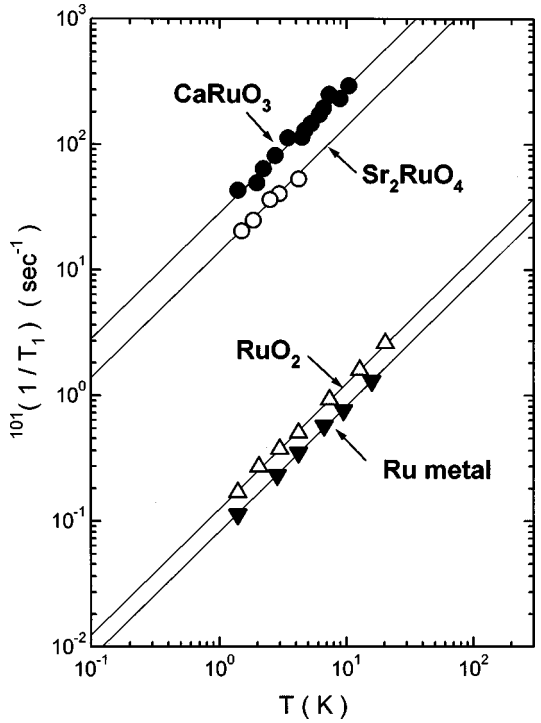

FIG. 6. T dependence of $^{101}(1/T_1)$ for Ru metal, RuO_2, and $CaRuO_3$ together with that for Sr_2RuO_4 (Ref. 15). $^{101}(1/T_1)$ in RuO_2 is estimated from the experimental values of $^{99}(1/T_1)$ using the relation of $(^{101}\gamma_n/^{99}\gamma_n)^2 \cdot {}^{99}(1/T_1)$. $^{101}(1/T_1)$ in Sr_2RuO_4 is the isotropic component of $^{101}(1/T_1)_{ab,c}$ (Ref. 15). $^{101}(T_1T)^{-1}$'s in $CaRuO_3$ and Sr_2RuO_4 are two orders of magnitude larger than those values in Ru metal and RuO_2.

-162 kOe/μ_B (Rh metal), being close to $A_{hf}\sim -300 \pm 60$ kOe/μ_B in the FM state of $SrRuO_3$.

Using the spin part of Knight shift $K_d \approx -25\%$ at 4.2 K and A_{hf} in $CaRuO_3$, it should be noted that a ratio of $\chi_d/\chi_{band}=1/(1-\alpha)\approx 58.8$ is strongly exchange enhanced. Here χ_d and χ_{band} are the spin susceptibility estimated from K_d and the one calculated from the band calculation result,[22] respectively. A Stoner factor $\alpha \approx 0.98$ for $CaRuO_3$ is close to 1, entitling it as a nearly FM material.

It is noteworthy that the Knight shift for Sr_2RuO_4 lies on the same line of K_{obs} vs χ_{obs} plot as that for $CaRuO_3$ (Fig. 5). It suggests that $4d$ spins play vital roles on the magnetic and transport properties not only in $SrRuO_3$ and $CaRuO_3$ but also in Sr_2RuO_4.

2. Nuclear-spin-relaxation rate $1/T_1$

Figure 6 displays the T dependence of $^{101}(1/T_1)$ for $CaRuO_3$ at $H_{res}=12.6$ T in $T=1.4$–11 K together with the results for Sr_2RuO_4, Ru metal, and RuO_2. $^{101}(1/T_1)$ proportional to T has a large value of $^{101}(T_1T)^{-1}=28$ ($s^{-1}K^{-1}$). The constant values of $^{101}(T_1T)^{-1}$ for $CaRuO_3$ and Sr_2RuO_4 (Ref. 15) are two orders of magnitude larger than in the nonmagnetic Ru metal and RuO_2.

$(T_1T)^{-1}$ in ruthenium oxides is generally decomposed by the $5s$-spin, the $4d$-orbital, and the $4d$-spin contribution by the following relation:

$$\left(\frac{1}{T_1T}\right)_{obs}=\left(\frac{1}{T_1T}\right)_s+\left(\frac{1}{T_1T}\right)_{orb}+\left(\frac{1}{T_1T}\right)_d. \qquad (5)$$

A sum of $(T_1T)_s^{-1}$ and $(T_1T)_{orb}^{-1}$ is anticipated to be comparable to $^{101}(T_1T)_{obs}^{-1}=0.12$ (s^{-1} K^{-1}) in RuO_2, which is much smaller than $^{101}(T_1T)_{obs}^{-1}=28$ (s^{-1} K^{-1}). Furthermore, we estimate a value $^{101}(T_1T)_{orb}^{-1}\sim 0.18$ (s^{-1} K^{-1}) for $CaRuO_3$ from the following equation:

$$\left(\frac{1}{T_1T}\right)_{orb}=\pi k_B\gamma_n^2\hbar A_{orb}^2N^2(E_F)\frac{2}{3}f\left(2-\frac{5}{3}f\right), \qquad (6)$$

where $N_d(E_F)\sim 4.06$ (states/eV/cell/spin) from the band calculation,[22] $A_{orb}=2\mu_B\langle r^{-3}\rangle=385$ kOe/μ_B from the Hartree-Fock calculation of $\langle r^{-3}\rangle=4.2$ (a.u.) for free Ru^{4+} with the reduction factor of $\xi=3/4$,[23] and the fractional factor f due to the occupation of the t_{2g} orbits at the Fermi surface is $f=1$ in this case. Therefore it is evident that $(T_1T)_{obs}^{-1}$ for $CaRuO_3$ is dominated by the $4d$-spin contribution $(T_1T)_d^{-1}$.

In terms of the random-phase approximation (RPA), $(T_1T)_d^{-1}$ is described as

$$\left(\frac{1}{T_1T}\right)_d=\pi k_B\gamma_n^2\hbar K_d^2\left(\frac{1}{3}f^2+\frac{1}{2}(1-f^2)\right)R, \qquad (7)$$

where R is the correlation factor in a modified Korringa (MK) relation for exchange enhanced metals.[24,25] This factor is given by[26]

$$R=\left\langle\frac{(1-\alpha_0)^2}{(1-\alpha_{q_0})^2}\right\rangle_{FS}, \qquad (8)$$

where $\alpha_0=I\chi_0/2$, $\alpha_{q_0}=I\chi_0(q_0,0)/2$, and $\langle\cdots\rangle_{FS}$ means the average over the Fermi surface. Here $I=U/N_0$ with the intra-atomic Coulomb integral U and number of sites N_0, χ_0, and $\chi_0(q_0,\omega)$ is the noninteracting spin and dynamical susceptibility at $q=0$ and $q=q_0$, respectively. The value reflects intimately the q dependence of $\chi(q,0)$. In the case that ferromagnetic SF are significant with $\alpha_0\sim 1$, $R\ll 1$. In the case that antiferromagnetic SF play a crucial role, $R\gg 1$ for α_Q close to 1 where Q is the AF wave vector. In 2D exchange enhanced Pauli paramagnets where $\chi(q,0)$ exhibits a weak q dependence, $R\sim 1$ without depending on α_0.

Using $K_d\sim -25\%$ at $H_{res}=12.6$ T, $^{101}R\approx 0.15$ is obtained from Eq. (7). Various characteristic parameters in $CaRuO_3$ are summarized in Table I and compared with those in a nearly FM metal YCo_2. $\alpha\approx 0.98$ and $^{101}R\approx 0.15$ indicate that $CaRuO_3$ is closer to the FM instability than YCo_2 ($\alpha=0.95$ and $^{59}R=0.30$).[27] Note that $N_d(E_F)$ is smaller for $CaRuO_3$ than for YCo_2, whereas $\alpha=I\cdot N_d(E_F)$ is larger for the former than for the latter. It is concluded that the electron correlation in $CaRuO_3$ is stronger than in YCo_2. One may suppose that the large negative θ value in $CaRuO_3$ suggests a strong AFM interaction. Contrary to this expectation, a much smaller $^{101}R\approx 0.15$ and $\alpha\approx 0.98$ close to 1 evidence that $CaRuO_3$ is the 3D nearly FM metal dominated by SF with low frequencies and long-wavelength components.

E. Comparison with the magnetic properties in the superconducting Sr_2RuO_4

The NMR results for $CaRuO_3$ are compared with those for Sr_2RuO_4 (Ref. 15) with the similar RuO_6 octahedron.

TABLE I. Various characteristic parameters in Sr_2RuO_4 and $CaRuO_3$, together with those values of liquid ^{3}He at 27 bars (Ref. 30) and the nearly ferromagnetic YCo_2 (Ref. 27). The 2D nearly FM SF in Sr_2RuO_4 are distinguished from the 3D nearly FM SF with dominant low frequencies and long-wavelength components in $CaRuO_3$, YCo_2, and liquid ^{3}He.

	Sr_2RuO_4	$CaRuO_3$	^{3}He (Ref. 30)	YCo_2 (Ref. 31)
$N_d(E_F)$ (state/eV)	4.36 (Ref. 31)	4.06 (Ref. 22)		5.55
γ_{exp} (mJ/mol K^2)	39 (Ref. 1)	73 (Ref. 4)		36
γ_{band} (mJ/mol K^2)	10.3	9.54		13.0
$\gamma_{exp}/\gamma_{band}$	3.8	7.65	5.26	2.8
$\chi_{d,exp}$ (10^{-4} emu/mol)$_{T\to 0}$	9.7	77		35.4
$\chi_{d,band}$ (10^{-4} emu/mol)	1.41	1.31		1.79
$\chi_{d,exp}/\chi_{d,band}$	6.9	58.8	21	19.8
Wilson ratio; R_W	1.8	7.7	4	7.1
Stoner factor; α	0.86	0.98	0.95	0.95
$^{101}R_{ab}$	2.1	0.15		$^{59}R=0.30$
$^{101}R_c$	4.2	0.15		$^{59}R=0.30$
$^{17}R_{\parallel,\perp}$	0.8 (Ref. 26)			
$^{17}R_c$	11 (Ref. 26)			

The respective Stoner factors are $\alpha\approx 0.98$ and ≈ 0.86 for $CaRuO_3$ and Sr_2RuO_4, indicating that the magnetic susceptibility is more significantly enhanced than a respective value based on the band calculation. A substantial difference appears in ^{101}R as shown in Table I. Extremely small value of $^{101}R\approx 0.15$ and $\alpha\approx 0.98$ reveal that $CaRuO_3$ is a 3D nearly FM metal. By contrast, $^{101}R_{ab}\approx 2.1$ and $^{101}R_c\approx 4.2$ in Sr_2RuO_4 are even larger than 1, even though its Stoner factor points to the closeness to ferromagnetism. Here the *c*-axis component $^{101}R_c$ is about twice larger than the *ab*-plane component $^{101}R_{ab}$, suggesting that SF in Sr_2RuO_4 might be anisotropic. The result that $^{101}R_{ab,c}$ for Sr_2RuO_4 is larger than 1 demonstrates that the SF in Sr_2RuO_4 is different from those in the 3D nearly FM $CaRuO_3$ and/or liquid ^{3}He. It is also suggested from the fact that R_W in Sr_2RuO_4 is much smaller than in the 3D nearly ferromagnetic materials indicated in Table I.

Recently, ^{17}O-NMR studies in Sr_2RuO_4 clarified that there exists anisotropic SF in the RuO_2 plane.[26] At low temperatures, the in-plane components of the correlation factor $^{17}R_\perp\approx{}^{17}R_\parallel\approx 0.8$ are lower than and/or close to 1, whereas $CaRuO_3$ dominated by 3D-FM SF shows quite smaller than 1. The result indicates that the *in-plane* low-frequency components of the dynamical spin susceptibility $^{17}\chi''(q,\omega)_{\parallel,\perp}$, which is dominated by d_{xy} orbital character, are exchange enhanced with weak q dependence (2D nearly FM) as described in the above section. By contrast, its out-of-plane component $^{17}R_c\approx 11$ is one order of magnitude larger than in-plane components, indicating that the *out-of-plane* low-frequency component of the dynamical spin susceptibility $^{17}\chi''(q,\omega)_c$, which is dominated by $d_{xz,yz}$ orbital character, shows the development of AFM SF upon cooling below $T^*\sim 130$ K where the *c*-axis resistivity shows a metallic behavior.[26] Consequently, we concluded that 2D nearly FM SF is dominant in the RuO_2 plane, whereas interlayer AFM SF along the *c* axis below T^*. We propose that $^{101}R_{ab,c}>1$ may reflect some average on this highly anisotropic SF revealed by the ^{17}O-NMR measurements. This is because the H_{hf} at the Ru site is produced mainly by the isotropic inner-core polarization induced by $4d$ spins, which averages the SF at the Ru site. On the other hand, the H_{hf} at the O(1) site originates from the dipole interaction with spins on the $p\pi_\perp$ and $p\pi_c$ orbitals hybridized with the d_{xy} and $d_{xz,yz}$, respectively. This orbital dependent anisotropic hyperfine interaction at the O(1) sites enables us to probe the anisotropic SF. The existence of the *in-plane* FM SF is also evidenced by the identical T dependence between $^{17}(1/T_1)$ at the O(1) site and $^{101}(1/T_1)$ at the Ru site studied by Imai *et al.*[28]

Soon after the discovery of the superconductivity in Sr_2RuO_4, Rice and Sigrist proposed that Sr_2RuO_4 is the spin-triplet superconductor with analogy to the superfluid ^{3}He,[29] where the 3D-FM SF mediates a spin-triplet pair. However, as discussed above, the SF in Sr_2RuO_4 should be distinguished from the 3D-FM SF with dominant low frequencies and long-wavelength components, since exhibiting remarkable anisotropic SF. This anisotropic SF may be relevant to an orbital dependent electronic structure. The 2D nearly FM SF in the in-plane $4d_{xy}$-p_π band may play a significant role for the stabilization of parallel spin pairing state within the basal plane[2] among various representations of spin-triplet order parameter.

IV. CONCLUSIONS

We reported systematic Ru-NMR studies on the ferromagnetic $SrRuO_3$ and exchange enhanced paramagnetic $CaRuO_3$ as well as nonmagnetic Ru metal and RuO_2, and compared the obtained results with those in spin-triplet *p*-wave superconductor Sr_2RuO_4. The results for RuO_2 and Ru metal reveal that the Knight shift K_{obs} with a positive value of $\sim+1\%$ and the small nuclear-spin-lattice relaxation rate $^{101}(1/T_1)$ are not affected by the $4d$-spin contribution, but dominated by the $4d$-orbital and/or the $5s$-spin contributions. In $SrRuO_3$, the internal field at the Ru site in the ferromagnetic (FM) state below $T_C=160$ K is -329.6 kOe at $T\to 0$, and the negative hyperfine coupling constant $A_{hf}\sim -300\pm 60$ kOe/μ_B originates mainly from the inner-core polarization effect. In $CaRuO_3$ that is proved

to remain paramagnetic down to 1.4 K, the field H dependence of Knight shift $K_{obs}(H)$ is well scaled to the measured susceptibility with $A_{hf} \approx -222 \pm 50$ kOe/μ_B through the inner-core polarization. The spin susceptibility χ_d deduced from the Knight shift in $CaRuO_3$ is nearly two orders of magnitude larger than the value χ_{band} obtained from the band calculation. The Stoner factor $\alpha \approx 0.98$ is estimated from the ratio of $\chi_d/\chi_{band} \approx 58.8$, entitling $CaRuO_3$ as the nearly FM metal. The $^{101}(1/T_1)$ in $CaRuO_3$ comparable to that in Sr_2RuO_4 is two orders of magnitude larger than those values in Ru metal and RuO_2. This enhancement is due to the FM spin fluctuations (SF). From the modified-Korringa relation, the correlation factor $^{101}R \approx 0.15$ was deduced to be very small. $CaRuO_3$ was shown to be in the nearly FM regime, dominated by low-frequencies and long-wavelength SF components.

The anisotropic correlation factor ($^{101}R_{ab} \approx 2.1$ and $^{101}R_c \approx 4.2$) in Sr_2RuO_4 are one order of magnitude larger than $^{101}R \approx 0.15$ in $CaRuO_3$, nevertheless the Stoner factors for both materials point to the closeness to ferromagnetism. The results combined with the previous ^{17}O NMR study indicate that the *in-plane* low-frequency components of the dynamical spin susceptibility, which is dominated by d_{xy} orbital character, are exchange enhanced without any significant q dependence due to 2D electronic character (2D nearly-FM), by contrast, the *out-of-plane* low-frequency component of the dynamical spin susceptibility, which is dominated by $d_{xz,yz}$ orbital character, shows the existence of AFM SF between the layers at low temperature. Therefore we reinforce that the 2D nearly FM SF in Sr_2RuO_4 should be distinguished from the 3D low frequencies and long-wavelength FM SF in $CaRuO_3$. In this sense, the occurrence of spin-triplet p-wave superconductivity in Sr_2RuO_4 does not always originate from the 3D-FM SF with analogy to liquid ^{3}He. Alternatively, the 2D nearly FM SF in the in-plane $4d_{xy}$-p_π band may play a significant role for the stabilization of parallel spin pairing state within the basal planes among various representations of spin-triplet order parameter. These characteristic SF's provide an interesting scenario for the spin-triplet p-wave superconductivity in Sr_2RuO_4 that is mediated by the *in-plane* short-range SF with 2D nearly FM character based on the Hund's rule coupling between the d_{xy} and $d_{yz,zx}$ orbits.

ACKNOWLEDGMENTS

We thank I. Hase for informing us of the results of the band calculation in $CaRuO_3$, and Y. Maeno and S. Ikeda for valuable discussions and comments. We acknowledge the members of K. Amaya's laboratory in Osaka University for the use of a SQUID magnetometer. This work was supported by the COE Research (10CE2004) in a Grant-in-Aid for Scientific Research from the Ministry of Education, Sports, Science and Culture of Japan.

[1] Y. Maeno, H. Hashimoto, K. Yoshida, S. Nishizaki, T. Fujita, J. B. Bednorz, and F. Lichtenberg, Nature (London) **372**, 532 (1994).
[2] K. Ishida, H. Mukuda, Y. Kitaoka, K. Asayama, Z. Q. Mao, Y. Mori, and Y. Maeno, Nature (London) **396**, 658 (1998).
[3] H. Kobayashi, M. Nagata, R. Kanno, and Y. Kawamoto, Mater. Res. Bull. **29**, 1271 (1994).
[4] G. Cao, S. McCall, M. Shepard, J. E. Crow, and R. P. Guertin, Phys. Rev. B **56**, 321 (1997).
[5] A. Callaghan, C. W. Moeller, and R. Ward, Inorg. Chem. **5**, 1573 (1966).
[6] J. M. Longo, P. M. Raccah, and J. B. Goodenough, J. Appl. Phys. **39**, 1327 (1968).
[7] T. C. Gibb, R. Greatrex, N. N. Greenwood, and P. Kaspi, J. Chem. Soc. Dalton Trans. **1973**, 1250.
[8] A. Kanbayashi, J. Phys. Soc. Jpn. **44**, 108 (1978).
[9] S. Nakatsuji, S. Ikeda, and Y. Maeno, J. Phys. Soc. Jpn. **66**, 1868 (1997).
[10] S. Ikeda, Y. Maeno, and T. Fujita, Phys. Rev. B **57**, 978 (1998).
[11] G. Cao, S. McCall, and J. E. Crow, Phys. Rev. B **55**, R672 (1997).
[12] F. A. Cotton and J. T. Mague, Inorg. Chem. **5**, 317 (1966).
[13] H. Schäfer, G. Schneidereit, and W. Gerhardt, Z. Anorg. Allg. Chem. **319**, 327 (1963).
[14] J. M. Fletcher, W. E. Gardner, B. F. Greenfield, M. J. Holdoway, and M. H. Rand, J. Chem. Soc. A **1968**, 653.
[15] K. Ishida, Y. Kitaoka, K. Asayama, S. Ikeda, S. Nishizaki, Y. Maeno, K. Yoshida, and T. Fujita, Phys. Rev. B **56**, R505 (1997).
[16] A. Narath, Phys. Rev. **162**, 320 (1967).
[17] A. Burgstaller, J. Voitlander, and H. Ebert, J. Phys.: Condens. Matter **6**, 8335 (1994).
[18] C. E. Boman, Acta Chem. Scand. **24**, 116 (1970).
[19] K. M. Glassford and J. R. Chelikowsky, Phys. Rev. B **47**, 1732 (1993).
[20] T. Kiyama, K. Yoshimura, K. Kosuge, Y. Ikeda, and Y. Bando, Phys. Rev. B **54**, R756 (1996).
[21] M. Kontani, T. Hiroi, and Y. Masuda, J. Phys. Soc. Jpn. **32**, 416 (1972).
[22] I. Hase *et al.* (unpublished).
[23] A. J. Freemann and R. E. Watson, in *Magnetism*, edited by G. T. Rado and H. Suhl (Academic, New York, 1965), Vol. II A, p. 167.
[24] T. Moriya, J. Phys. Soc. Jpn. **18**, 516 (1963).
[25] A. Narath and H. T. Weaver, Phys. Rev. **175**, 373 (1968).
[26] H. Mukuda, K. Ishida, Y. Kitaoka, K. Asayama, Z. Mao, Y. Mori, and Y. Maeno, J. Phys. Soc. Jpn. **67**, 3945 (1998).
[27] K. Yoshimura, M. Mekata, M. Takigawa, Y. Takahashi, and H. Yasuoka, Phys. Rev. B **37**, 3593 (1988).
[28] T. Imai, A. W. Hunt, K. R. Thurber, and F. C. Chou, Phys. Rev. Lett. **81**, 3006 (1998).
[29] T. M. Rice and M. Sigrist, J. Phys.: Condens. Matter **7**, L643 (1995).
[30] W. R. Abel, A. C. Anderson, and J. C. Wheatley, Phys. Rev. Lett. **17**, 74 (1966).
[31] T. Oguchi, Phys. Rev. B **51**, 1385 (1995).